Cranfield Memo. No. 9

CRANFIELD INSTITUTE OF TECHNOLOGY

Department of Aircraft Design

DESIGN CHARTS FOR CARBON FIBRE COMPOSITES

by

R. Tetlow

Cranfield Memo No.9

Cranfield Institute of Technology

DESIGN CHARTS FOR CARBON FIBRE COMPOSITES

by R. Tetlow,D.C.Ae.,A.F.R.Ae.S.,C.Eng.

Department of Aircraft Design

SUMMARY

This report contains charts of elastic properties and buckling coefficients of a simply supported compression panel, based on theory of multi layer plates of orthotropic material, for a typical carbon fibre composite. In addition the optimum orientation of plies, of a three ply system, is considered for a corrugated compression panel together with the modifications necessary for other panel shapes. The computer programmes used are contained in the Appendix.

Work carried out as part fulfilment of MinTech contract no. PD/28/040 'Application of Carbon Fibre Composite to an Airbus'.

CONTENTS

LIST OF FIGURES

NOTATION

$D_{1,2}$	flexural rigidity (eq.4a)
E	elastic modulus
F	
F	efficiency factor (eq.5n)
G	shear modulus
K	buckling coefficient
K'	buckling coefficient of composite plate (eq.4d)
L	strut length
M	panel geometry parameter (eq.5l)
N	$a/b(D_2/D_1)^{1/4}$
R	angle ply thickness/total thickness
S	measured shear strength of single ply.
V_f	filament volume fraction
X	measured longitudinal strength of single ply
Y	measured transverse strength of single ply
Z	material parameter (eq.5l)
a_{11}, a_{22}	flexibility coefficients of single layer (eq.2c)
b_{11}, b_{22}	stiffness coefficients of single layer (eq.2b)
a	plate length
b	plate width
r_{11}, r_{22}	flexibility coefficients of total composite (eq.3b)
t	plate thickness
$\bar{t}$	effective thickness (eq.5d)
w	end load/in.
ϵ	direct strain
γ	shear strain
θ	ply angle (fig.2)
ϕ	corrugation angle (fig.9)
μ	Poisson's ratio
σ	direct stress
τ	shear stress

Notation ctd.

Subscripts

A	applied
C	compression
T	tension
CR	buckling
LI	local instability
LW	long wave
f	flank
c	crest
x,y,z	applied stress axes
α,β,γ	filamentary axes
o	longitudinal axis of single ply.

1. Introduction

The increasing availability of high strength and stiffness, lightweight filaments and in particular carbon fibre has led to a study of the potential structural weight saving with this new material. In the course of this work the need for methods of selecting the most suitable orientation of multi-layer composites, for various types of loading, became apparent. Techniques similar to those used for predicting the behaviour of plywood and glass reinforced plastics have been used.

The results are presented as follows,

i) graphs of elastic and strength properties together with a computer programme with which it is possible to select layups suitable for combined loading conditions

ii) a chart of buckling coefficients for a simply supported panel, together with the modification necessary for other edge conditions

iii) a design chart for a corrugated compression panel.

The material chosen for the study was a high modulus carbon fibre composite with a 60 per cent filament volume. However the results can be modified for other materials.

2.0 Elastic Properties

Methods of predicting the elastic properties of a single uni directional laminate from the properties of its constituents, are available, but all rely on a knowledge of the void content, straightness of filaments, etc. Data regarding these properties is practically non-existent for carbon composites hence the measured elastic properties of a single sheet of composite have been used. The fibre content chosen was 60 per cent by volume as this appears to be approaching a working maximum, further increases resulting in a marked reduction in transverse strength and stiffness.

The properties used were as follows:-

Material - Fibre: Type I High Modulus, treated
Resin: Epoxy

$V_f = 0.60$

$E_\alpha = 30 \times 10^6$ lb/in^2

$E_\beta = 1.1 \times 10^6$ lb/in^2

$G_{\alpha\beta} = 0.7 \times 10^6$ lb/in^2

$\mu_{\alpha\beta} = 0.3$

Methods of determining the elastic properties of multi-directional laminates are well established (ref.1) and have been used with success for plywoods and glass laminates.

2.1 General relationship for orthotropic laminates

Each layer has three moduli of elasticity in the direction of the three axes (see fig.1) one of which is parallel to the filaments, three moduli of rigidity $G_{\alpha\beta}$, $G_{\beta\alpha}$, $G_{\gamma\alpha}$ and six Poisson's ratios, two associated with each axis, $\mu_{\alpha\beta}$, etc. The latter are not independent but are associated as follows

$$\left.\begin{aligned} \frac{\mu_{\alpha\beta}}{E_\alpha} &= \frac{\mu_{\beta\alpha}}{E_\beta} \\ \frac{\mu_{\alpha\gamma}}{E_\alpha} &= \frac{\mu_{\gamma\alpha}}{E_\gamma} \\ \frac{\mu_{\beta\gamma}}{E_\beta} &= \frac{\mu_{\gamma\beta}}{E_\gamma} \end{aligned}\right\} \quad \ldots (2a)$$

It thus requires nine independent properties to completely define the elastic behaviour of an anisotropic material. For sheet materials it is normal to assume (ref.1) that

$E_\gamma = E_\beta$, $G_{\beta\gamma} = G_{\alpha\gamma} = G_{\alpha\beta}$, $\mu_{\beta\gamma} = \mu_{\gamma\beta} = \mu_{\alpha\gamma}$

this reduces the required number of elastic constants to E_α, E_β, $G_{\alpha\beta}$, $\mu_{\alpha\beta}$.

2.2 Stress-strain relationship

Consider now the effect of rotating the filamentary axes, α,β through an angle θ with respect to the axes of applied stress, x, y (see fig.2).

It can be shown that (ref.1)

$$\begin{bmatrix}\sigma_x\\ \sigma_y\\ \tau_{xy}\end{bmatrix} = \left[b_{ij}\right] \begin{bmatrix}\epsilon_x\\ \epsilon_y\\ \gamma_{xy}\end{bmatrix} \qquad \ldots (2b)$$

where $b_{11} = \frac{1}{\lambda}\left[E_\alpha\cos^4\theta + E_\beta\sin^4\theta + \sin^2\theta\cos^2\theta(2E_\alpha\mu_{\beta\alpha} + 4\lambda G_{\alpha\beta})\right]$

$b_{22} = \frac{1}{\lambda}\left[E_\beta\cos^4\theta + E_\alpha\sin^4\theta + \sin^2\theta\cos^2\theta(2E_\alpha\mu_{\beta\alpha} + 4\lambda G_{\alpha\beta})\right]$

$b_{33} = \frac{1}{\lambda}\left[\sin^2\theta\cos^2\theta(E_\alpha + E_\beta - 2E_\alpha\mu_{\beta\alpha}) + \lambda G_{\alpha\beta}(\cos^2\theta - \sin^2\theta)^2\right]$

$b_{21} = b_{12} = \frac{1}{\lambda}\left[\sin^2\theta\cos^2\theta(E_\alpha + E_\beta - 4\lambda G_{\alpha\beta}) + E_\alpha\mu_{\beta\alpha}(\cos^4\theta + \sin^4\theta)\right]$

$b_{31} = b_{13} = \frac{1}{\lambda}\left[\sin^3\theta\cos\theta(E_\beta - E_\alpha\mu_{\beta\alpha} - 2\lambda G_{\alpha\beta}) - \sin\theta\cos^3\theta (E_\alpha - E_\alpha\mu_{\beta\alpha} - 2\lambda G_{\alpha\beta})\right]$

$b_{32} = b_{23} = \frac{1}{\lambda}\left[\sin\theta\cos^3\theta(E_\beta - E_\alpha\mu_{\beta\alpha} - 2\lambda G_{\alpha\beta}) - \sin^3\theta\cos\theta (E_\alpha - E_\alpha\mu_{\beta\alpha} - 2\lambda G_{\alpha\beta})\right]$

where $\lambda = 1 - \mu_{\beta\alpha}\mu_{\alpha\beta}$

and also by inversion

$$\begin{bmatrix}\epsilon_x\\ \epsilon_y\\ \gamma_{xy}\end{bmatrix} = \left[a_{ij}\right]\begin{bmatrix}\sigma_x\\ \sigma_y\\ \tau_{xy}\end{bmatrix} = \left[b_{ij}\right]^{-1}\begin{bmatrix}\sigma_x\\ \sigma_y\\ \tau_{xy}\end{bmatrix} \qquad \ldots (2c)$$

where $\mu_{xy} = -\frac{a_{12}}{a_{11}}$; $\mu_{yx} = -\frac{a_{12}}{a_{22}}$

$E_x = \frac{1}{a_{11}}$; $E_y = \frac{1}{a_{22}}$; $\sigma_{xy} = \frac{1}{a_{33}}$

2.3 Laminated composites

Only 'balanced' laminates are considered, that is plates that have a symmetrical distribution of plies about the median plane. The plates do not therefore twist when subjected to in plane forces or bending moments. (See fig.2)

a) Plate Stretching

$$b_{11\ COMP} = \frac{1}{t} \sum_{i=1}^{i=n} b_{11_i} t_i \qquad \ldots (2d)$$

etc.

b) Plate Bending

$$b_{11\ COMP} = \frac{1}{I} \sum_{i=1}^{i=n} b_{11_i} I_i \qquad \ldots (2e)$$

etc.

Inversion of the b_{ij} matrix for the composite will yield the composite elastic moduli.

For this study the number of layers has been assumed to be large, as thin prepregs (.001") are available and the effect of asymmetry could be minimised. Consequently eq.(2d) has been used to calculate the laminate properties. This was achieved with the use of an ICL 1905 computer together with a simple program in JEAN language. The results are tabulated for various values of cross ply angle (θ) and proportion of cross plies (R), (App.1). The results are also plotted in figs. 3, 4 and 5. It will be noted that with R = 1.0 (i.e. all cross plies) at small angles (say 10^o) $\mu_{xy} > 1.0$. This is verified by Cox (ref.2) and although it is not calculated would be accompanied by an appropriate Poisson's ratio μ_{xz} through thickness of the laminate in order that the volume of the plate does not change. This is also borne out by Rothwell (ref.3) for a similar layup.

3.0 Strength of Multi Layer Composites

Methods of predicting the strength of uni-directional sheets based on the constituent properties have been suggested (ref.4). However for practical purposes the values obtained are dubious in that they rely on a knowledge of the void content, arrangement of fibres, etc. Consequently measured unidirectional sheet strength properties have been used in this analysis. Very little experimental data is available on the behaviour of carbon composites loaded at axes other than the filamentary axes.

The data used is based on the same material as that used in Appendix 1 and the measured strength values used were as follows

X_T = 150,000 lb/in^2 tension

X_C = 120,000 lb/in^2 compression

Y = 6,000 lb/in^2 tension and compression

S = 8,000 lb/in^2.

3.1 Theoretical analysis

Failure criteria are discussed in detail by TSAI (ref.4) and by Chamis (ref.5). The most effective method appears to be that proposed by Hill (ref.6) for an anisotropic material.

The criterion used is

$$K = \frac{X}{\sqrt{\sigma_\alpha^2 - \sigma_\alpha \cdot \sigma_\beta + \frac{X^2}{Y^2} \cdot \sigma_\beta^2 + \frac{X^2}{S^2} \cdot \tau_{\alpha\beta}^2}} \qquad \ldots (3a)$$

where X, Y, and S are the measured longitudinal transverse and shear strengths respectively.

Consider now the stresses applied to a multi layer composite.

$$\begin{bmatrix} \epsilon_x \\ \epsilon_y \\ \gamma_{xy} \end{bmatrix}_{COMP} = \left[b_{ij}\right]^{-1}_{COMP} \begin{bmatrix} \sigma_x \\ \sigma_y \\ \tau_{xy} \end{bmatrix} = \left[a_{ij}\right]_{COMP} \begin{bmatrix} \sigma_x \\ \sigma_y \\ \tau_{xy} \end{bmatrix}$$

$$= \left[r_{ij}\right] \begin{bmatrix} \sigma_x \\ \sigma_y \\ \tau_{xy} \end{bmatrix} \qquad (3b)$$

Then using the strains calculated above stresses in a layer of the composite can be calculated

$$\therefore \quad \begin{bmatrix} \sigma_x \\ \sigma_y \\ \tau_{xy} \end{bmatrix}_{LAYER} = \left[b_{ij_{LAYER}}\right] \left[r_{ij}\right] \begin{bmatrix} \sigma_x \\ \sigma_y \\ \tau_{xy} \end{bmatrix}_{COMP} \quad \ldots (3c)$$

In order that these may be applied to the failure criterion then these stresses must be transferred to the filamentary axes of the layer, hence:

$$\begin{bmatrix} \sigma_\alpha \\ \sigma_\beta \\ \tau_{\alpha\beta} \end{bmatrix}_{LAYER} = \left[mn\right] \left[b_{ij_{LAYER}}\right] \left[r_{ij}\right] \begin{bmatrix} \sigma_x \\ \sigma_y \\ \tau_{xy} \end{bmatrix}_{COMP} \quad (3d)$$

where $$\left[mn\right] = \begin{bmatrix} \cos^2\theta, & \sin^2\theta, & -2\sin\theta\cos\theta \\ \sin^2\theta, & \cos^2\theta, & 2\sin\theta\cos\theta \\ \sin\theta\cos\theta, & -\sin\theta\cos\theta, & (\cos^2\theta - \sin^2\theta) \end{bmatrix}$$

These stresses can then be substituted into the chosen strength criterion and the strength factor K determined. Failure will obviously occur in one of the layers and if required further analysis could be carried out to determine final strength of the laminate without the failed layer. This latter exercise has not been attempted as it was felt that for components subjected to a complex stress system almost invariably the remaining layers would be incapable of supporting the stresses imposed and total failure would occur. For simple tension however it might be possible to use the initial failure as a proof load but it is very unlikely to be of practical value.

The analysis has been carried out for various ratios of applied stresses and the results are shown in figs. 6 and 7 for simple tension and compression.

The analysis was achieved by use of an ICL 1905 and a Fortran IV computer program. This is listed in App.2. As the data and programs are on cards, substitution of new data and deletion of WRITE statements where not required is simple. Using this program and by substitution of appropriate values of σ_x, σ_y, and τ_{xy} (i.e. applied stress system) it is possible to determine the best layup, based on maximum strength, for a 3-fibre system. The program is being modified to include other types of layup (e.g. a 4-fibre system) and to allow for possible assymetry.

4.0 Buckling of Plates

The theoretical analysis of the buckling of anisotropic plates in compression and shear is well established (ref.7) and in the case of plywood and G.R.P. plates has been verified experimentally (ref. 8, 9). Experimental testing has been carried out at the College as part of student theses (ref.10, 11) and results indicate the theory is applicable to C.F. composites.

4.1 Buckling in compression of simply supported orthotropic plates

An expression for the buckling stress of an orthotropic plate is derived in ref.12 as shown below.

$$\sigma_{CR} = \frac{2\pi^2}{b^2 t}\left[(D_1 D_2)^{1/2} + D_3\right] \qquad \ldots (4a)$$

where D_1 = flexural rigidity corresponding to bending moment M_x

$= (EI)_x/\lambda$

D_2 = flexural rigidity corresponding to bending moment M_y

$= (EI)_y/\lambda$

$D_3 = \frac{1}{2}(\mu_{xy}.D_2 + \mu_{yx}.D_1) + 2(GI)_{xy}$

where $(GI)_{xy}$ is the average torsional rigidity of the plate.

$\lambda = 1 - \mu_{xy}.\mu_{yx}$

For a thin plate, thickness t, these stiffnesses may be expressed as (ref.12)

$$\begin{aligned} D_1 &= E_x.t^3/12\lambda \\ D_2 &= E_y.t^3/12\lambda \qquad \ldots (4b) \\ D_3 &= t^3(\mu_{xy}.E_y + \mu_{yx}.E_x)/24\lambda + t^3 G_{xy}/6 \end{aligned}$$

Then substituting (4b) into (4a) gives

$$\sigma_{CR} = \frac{\pi^2}{6\lambda}\left[(E_x.E_y)^{1/2} + \mu_{xy}.E_y/2 + \mu_{yx}.E_x/2 + 2\lambda G_{xy}\right] x\left[\frac{t}{b}\right]^2 \qquad \ldots (4c)$$

or $\sigma_{CR} = E_{xo}\,(K')\left(\frac{t}{b}\right)^2 \qquad \ldots (4d)$

where E_{xo} = longitudinal modulus of a single unidirectional sheet.

$$K' = \frac{1}{E_{xo}} \cdot \frac{\pi^2}{6\lambda} \left[(E_x . E_y)^{1/2} + \mu_{xy} E_y/2 + \mu_{yx} . E_x/2 + 2\lambda G_{xy} \right]$$

The expression K' has been evaluated in the JEAN programme used in App.1 for plates with a balanced layup and the results are plotted in fig. 8 . It can be seen that the optimum layup for plate buckling occurs when R = 1.0 (all angle ply), $\theta = 45^{\circ}$. However the permissible compressive stress for this layup is only 15,000 psi. compared with a maximum possible of 120,000 psi for unidirectional material.

It can be shown that the optimum stress level,

$$\sigma_{OPT} = \sqrt[3]{E_{xo} . K'} \left(\frac{P}{b^2} \right)^{2/3} \qquad \ldots (4e)$$

where P = applied compressive load

$\frac{P}{b^2}$ = structural index.

As the structural index is increased it will be necessary to introduce an increasing number of axial plies or angle plies at a small angle, θ, in order to increase the optimum stress level. By superimposing lines of constant stress from fig.9 on the chart for buckling coefficient, K' (fig. 9) a 'path to follow' from the optimum layup (i.e. R = 1.0, $\theta = 45^{\circ}$) may be determined. This is shown as a dotted line on fig. 8 .

Fig.10 shows optimum stress level vs. structural index for carbon fibre composite compared with steel and aluminium alloy.

The buckling chart, fig.8 may also be used to determine the buckling coefficient for plates with different edge conditions and aspect ratios. Wittrick (ref.13) has suggested that the buckling curves in ref.14 which give buckling coefficient K versus a/b (panel aspect ratio) for various edge conditions may be used by substituting a value

$$N = \frac{a}{b} . \left(\frac{D_2}{D_1} \right)^{1/4} \quad \text{for aspect ratio } a/b$$

Then buckling stress,

$$\sigma_{CR} = \frac{K_R . Ae . S .}{3.62} . K' \left(\frac{t}{b} \right)^2 \qquad \ldots (4f)$$

5.0 Design of Wide Compression Panels

Optimum design procedures for wide panels subjected to compressive loading almost invariably establish a design criteria that all modes of buckling occur simultaneously. The procedure adopted in this section is similar in that local and long wave instability modes are assumed to be coincident. The types of panels considered do not buckle in the torsional mode and in fact types of construction prone to this mode of buckling appear to be unattractive in filamentary composites for most purposes.

5.1 Corrugated compression panels

Consider the buckling of a corrugated compression panel (see fig.11), the modes of buckling to be anticipated are

i) local buckling of plate elements
ii) long wave buckling of whole panel.

For i) the plate is assumed to be simply supported and infinitely long, although if necessary the interaction effect with the adjacent plates could be included and for ii) ends of the panel are assumed to be simply supported.

In this initial analysis the column is assumed to be made from a constant thickness sheet where

$$t_c = t_f = t; \quad b_c = b_f = b \qquad \ldots (5a)$$

Then local buckling stress of plate,

$$\sigma_{LI} = E_{xo}(K')\left(\frac{t}{b}\right)^2 \qquad \ldots (5b)$$

where E_{xo} and (K') are defined in 4.1.

Long wave buckling stress of panel,

$$\sigma_{LW} = \frac{\pi^2 E_x . I}{L^2 \bar{t}} \qquad \ldots (5c)$$

where $$\bar{t} = \frac{2t}{(1 + \cos\phi)} \qquad \ldots (5d)$$

$$I = \left[2bt\left(\frac{h}{2}\right)^2 + \frac{2t}{\sin\phi} \cdot \frac{h^3}{12}\right] \cdot \frac{1}{2b(1 + \cos\phi)} \qquad \ldots (5e)$$

for $0 < \phi < 120^\circ$

$$h = b \sin\phi \qquad \ldots (5f)$$

Substituting (5f) into(5e) we obtain

$$I = \frac{1}{3} \frac{b^2 t \sin^2\phi}{(1 + \cos\phi)} \qquad \ldots (5g)$$

and by substituting (5g) and (5d) into (5e) we obtain

$$\sigma_{LW} = \frac{\pi^2 . E_x . \sin^2\phi}{6} \cdot \frac{b^2}{L^2} \qquad \ldots (5h)$$

now applied stress,

$$\sigma_A = \frac{\omega}{\bar{t}} = \frac{\omega(h\ \cos\phi)}{2t} \qquad \ldots (5i)$$

As all buckling modes occur simultaneously

$$\sigma_{LI} = \sigma_{LW} = \sigma_A = \sigma \qquad \ldots (5j)$$

and by examining equations (5b),(5c) and (5h) we can show

$$\sigma^4 = \sigma_{LI} \cdot \sigma_{LW} \cdot \sigma_A^2 = \frac{\pi^2 . E_x \sin^2\phi}{6} \cdot \frac{b^2}{L^2} \cdot E_{xo}(K')\left(\frac{t}{b}\right)^2 \times \frac{\omega^2}{4t^2}(1 + \cos\phi)^2$$

Rearranging this becomes

$$\sigma^4 = \frac{\pi^2}{24}\left[E_x . E_{xo}(K')\right]\left[\sin^2\phi(1+\cos\phi)^2\right]\left[\frac{\omega}{L}\right]^2 \qquad \ldots (5k)$$

or

$$\sigma^4 = \frac{\pi^2}{24} . E_{xo}^2 . Z . M . \left[\frac{\omega}{L}\right]^2 \qquad \ldots (5l)$$

where $Z = \dfrac{E_x . E_{xo} . K'}{E_{xo}^2}$

$$M = \sin^2\phi(1 + \cos\phi)^2$$

By examining eq.(5l) it can be seen that the parameters for material properties, Z and cross sectional geometry, M are independent and for a given loading index, ω/L may be maximised separately in order to achieve the maximum stress, σ and hence the lightest panel. The maximum value of M occurs when $\phi = 60^0$ and substituting this value into eq.(5l) yields

$$\sigma = 0.914 \sqrt[4]{E_{xo}^2 \cdot Z} \sqrt{\omega/L} \qquad \ldots (5m)$$

The material property parameter, Z has been evaluated in the JEAN programme in App.1 and the results are shown in fig.12. It can be seen that the maximum value of Z occurs when R = 0.33, θ = 55. This 'optimum' orientation will only apply up to the stress level that can be achieved by this particular configuration. In order to increase the stress level (i.e. at a higher loading index, ω/L) then the layu must be altered and the 'path to follow' from the optimum is obtained as in 4.0 by superposition of lines of constant allowable stress and the path is shown on fig.12. By following this path a graph of optimum stress level, σ_{OPT} versus loading index, ω/L may be constructed and is shown in fig.13 in comparison with aluminium alloy.

When the material considered is isotropic i.e. $E_x = E_{xo}$ = E etc. eq.(5m) becomes

$$\sigma = F \sqrt{E} \sqrt{\omega/L} \qquad \ldots (5n)$$

where F = Efficiency Factor (= 1.26 for corrugated panel) and this agrees with the expression obtained by Emero and Spunt (Ref.15)

For other cross sectional shapes it is suggested that eq.(5m) can be modified as follows

$$\sigma = 0.914 \sqrt[4]{E_{xo}^2 \cdot Z} \cdot \sqrt{\frac{\omega}{L}} \cdot \frac{F'}{1.26} \qquad \ldots (5p)$$

where F' = Efficiency Factor of panel (see table 1) However this will only apply to panels prone to similar modes of failure (i.e. no torsional instability)

6.0 Conclusions

Before attempting to use these highly anisotropic materials careful consideration must be given not only to the type, magnitude and variations in the applied loadings but also to the design specifications. Merely attempting to substitute carbon fibre for metal and expecting exactly similar performance will not realise the full potential of the material.

The methods presented should be useful as a guide for designers faced with selecting fibre orientations for the chosen material. They will also serve as a guideline for similar highly anisotropic materials as the buckling charts are presented in terms of the longitudinal elastic modulus of a single ply.

It is proposed to extend the work and to present a family of charts to include materials with less marked anisotropy eg. glass fibre. If required the methods and computer programme are also suitable with little modification for use with composites composed of layers of different materials.

REFERENCES

1. - Plastics for Aircraft, Pt.1, Reinforced Plastics. ANC-17.

2. Cox, H.L. The Elasticity and Strength of Paper and other Fibrous Materials. British Journal of Applied Physics, 18 May 1951.

3. Rothwell, A. Optimum Fibre Orientation for the Buckling of Thin Plates of Composite Material. Fibre Science and Technology, Oct. 1969.

4. Tsai, S. Strength Characteristics of Composite Materials. NASA CR-224 April 1965.

5. Chamis, C.C. Failure Criteria for Filamentary Composites NASA TN D-5367, Aug. 1969.

6. Hill, R. The Mathematical Theory of Plasticity Clarendon Press, Oxford 1950.

7. Dietz, A.G.H. (ed.) Engineering Laminates, Chap.1 by N.J. Hoff. John Wiley and Sons, 1949.

8. Wooden Aircraft Structures
ANC-18

9. Davis, J.G. and Zender, G.W. Compressive Behaviour of Plates Fabricated from Glass Filaments and Epoxy Resin.
NASA TN D-3918, April 1967.

10. Harris, C.M. Buckling of Fibre Reinforced Plastic Plates.
College of Aeronautics Thesis, Sept.1968.

11. Brain, C.J. Buckling of Filament Reinforced Plastic Plates.
College of Aeronautics Thesis, Sept.1969.

12. Timoshenko, S.P. and Gere, J.M. Theory of Elastic Stability.
McGraw-Hill, 1961.

13. Wittrick, W.H. Correlation Between Some Stability Problems for Orthotropic and Isotropic Plates Under Bi-axial and Uni-Axial Direct Stress.
Aero. Quarterly, Vol.4, 1952-54.

14. - R.Ae.Soc. Structures Data Sheet 02.01.01.

15. Emero, D.H. and Spunt, L. Optimisation of Multirib and Multiweb Wing Box Structures under Shear and Moment Loads.
A.I.A.A. 6th Structures and Materials Conference, Palm Springs, Calif. April 65.

APPENDIX 1 - Evaluation of Elastic Properties and Buckling Coefficients

```
THIS IS A JEAN PROGRAMME FOR EVALUATING THE BIJ MATRIX

 1.0 TYPE "B11"
 1.1 SET Z=M*COS(A)↑4+N*SIN(A)↑4
 1.2 SET Y=[Z+SIN(A)↑2*COS(A)↑2*(2*M*U+4*S*R)]/S
 1.3 TYPE Y
 2.0 TYPE "B22"
 2.1 SET X=N*COS(A)↑4+M*SIN(A)↑4
 2.2 SET W=[X+SIN(A)↑2*COS(A)↑2*(2*M*U+4*S*R)]/S
 2.3 TYPE W
 3.0 TYPE"B33"
 3.1 SET V=SIN(A)↑2*COS(A)↑2*(M+N-2*M*U)
 3.2 SET J=[V+S*R*(COS(A)↑4-2*SIN(A)↑2*COS(A)↑2+SIN(A)↑4)]/S
 3.3 TYPE J
 4.0 TYPE "B12"
 4.1 SET C=SIN(A)↑2*COS(A)↑2*(M+N-4*S*R)
 4.2 SET D=[C+M*U)*(COS(A)↑4+SIN(A)↑4)]/S
 4.3 TYPE D
 5.0 TYPE "B13"
 5.1 SET E=SIN(A)↑3*COS(A)*(N-M*U-2*S*R)
 5.2 SET F=[E-SIN(A)*COS(A)↑3*(M-M*U-2*S*R)]/S
 5.3 TYPE F
 6.0 TYPE "B32"
 6.1 SET G=SIN(A)*COS(A)↑3*(N-M*U-2*S*R)
 6.2 SET H=[G-SIN(A)↑3*COS(A)*(M-M*U-2*S*R)]/S
 6.3 TYPE H
```

Results of JEAN Programme I

θ	B_{11}	B_{22}	B_{33}	B_{12}	B_{13}	B_{23}
0°	30.09932778	1.103642019	.7	.3310926056	0	0
10°	28.41373704	1.166705089	1.511263838	1.142356444	-4.708206227	-.250348073
20°	23.84202089	1.630036936	3.565455987	3.196548593	-8.074434353	-1.244599418
30°	17.64900923	3.151166349	5.90139711	5.532489716	-9.28077814	-3.274722096
40°	11.3929345	6.357886508	7.426074396	7.057167001	-8.324782427	-5.952805646
50°	6.357886509	11.3929345	7.426074396	7.057167001	-5.952805646	-8.324782426
60°	3.151166349	17.64900923	5.901397111	5.532489717	-3.274722096	-9.28077814
70°	1.630036937	23.84202089	3.565455988	3.196548593	-1.244599419	-8.074434354
80°	1.166705089	28.41373703	1.511263839	1.142356444	-.2503480731	-4.708206228
90°	1.103642019	30.09932778	.7	.3310926056	-4.302697535&-11	-1.945331443&-9
45°	8.666288753	8.666288752	7.635196147	7.266288753	-7.248921441	-7.248921441

-SET M=30.0 E_α
-SET N=1.1 E_β
-SET Q=0.011 $\mu_{\beta\alpha}$
-SET R=0.7 $G_{\alpha\beta}$

JEAN Programme 2 - Buckling Coefficients

```
2.00 SET M=A+(E-A)*R
2.01 SET N=B+(F-B)*R
2.02 SET □=C+(G-C)*R
2.03 SET P=D+(H-D)*R
2.04 SET Q=M*N*□-P↑2*□
2.05 SET S=N*□/Q
2.06 SET T=M*□/Q
2.07 SET U=(M*N-P↑2)/Q
2.08 SET V=P*□/Q
2.09 TYPE R IN FORM 1
2.10 SET W=1/S
2.11 SET X=1/T
2.12 SET Y=1/U
2.13 SET I=V/S
2.14 SET J=V/T
2.15 TYPE W,X,Y,I,J IN FORM 2
2.16 SET K=[W↑0.5*X↑0.5+I*X/2+J*W/2+2*Y*(1-I*J)]
2.17 SET K=K*1.6499/(1-I*J)
2.19 SET Q=K/30          Q = K'
2.20 TYPE Q IN FORM 3
2.21 SET Z=W*K/900
2.22 TYPE Z IN FORM 4
```

A = B11
B = B22
C = B33
D = B12
0°Ply

E = B11
F = B22
G = B33
H = B12
Cross Ply

R = Cross Ply Ratio

Set of Typical Results for Jean Programme 2

$\theta = 10^{o}$

```
←SET E=28.414
←SET F=1.1667
←SET G=1.5113
←SET H=1.1424
←DO PART 2 FOR R=0(0.1)1.0
 .000
30.000    1.100    .7000    .3000    .0110
 .4122
 .4122
 .100
29.777    1.104    .7811    .3714    .0138
 .4256
 .4224
 .200
29.544    1.108    .8623    .4420    .0166
 .4390
 .4323
 .300
29.299    1.111    .9434    .5118    .0194
 .4523
 .4418
 .400
29.044    1.114   1.0245    .5808    .0223
 .4657
 .4509
 .500
28.778    1.117   1.1057    .6490    .0252
 .4791
 .4596
 .600
28.502    1.118   1.1868    .7165    .0281
 .4924
 .4678
 .700
28.215    1.120   1.2679    .7833    .0311
 .5058
 .4757
 .800
27.919    1.121   1.3490    .8493    .0341
 .5191
 .4831
 .900
27.612    1.121   1.4302    .9146    .0371
 .5324
 .4900
1.000
27.295    1.121   1.5113    .9792    .0402
 .5457
 .4965
```

APPENDIX 2 - FORTRAN Programme for Composite Strength

```
      MASTER COMPOSITE STRENGTH
      WRITE(2,1)
    1 FORMAT(28H  TETLOW COMPOSITE STRENGTH)
      READ(1,2)EA,EB,G,PB,BL,B110,B220,B330,B120
C EA IS EALPHA EB IS EBETA G IS SHEAR MOD PB IS MUBA BL IS LAMBDA
C SUFFIX 0 IN B TERMS REFERS TO ANGLE THETA
    2 FORMAT(9F0.0)
      READ(1,3)SX,SY,TXY
    3 FORMAT(3F0.0)
      DIMENSION R(10)
C R IS CROSS PLY RATIO
      DIMENSION T(10)
C T IS ANGLE THETA IN RADIANS
      READ(1,4)R
    4 FORMAT(10F0.0)
      READ(1,5)T
    5 FORMAT(10F0.0)
      WRITE(2,7)SX,SY,TXY
C SX,SY,TXY ARE APPLIED STRESSES USE 1000 AS MAX
    7 FORMAT(3F7.0)
      DO 61 I=1,10
      DO 62 N=1,10
      B11T=EA*COS(T(I))**4+EB*SIN(T(I))**4
      B11T=(B11T+(2.*EA*PB+4.*BL*G)*SIN(T(I))**2*COS(T(I))**2)/BL
      B22T=EB*COS(T(I))**4+EA*SIN(T(I))**4
      B22T=(B22T+(2.*EA*PB+4.*BL*G)*SIN(T(I))**2*COS(T(I))**2)/BL
      B33T=(EA+EB-2*EA*PB)*SIN(T(I))**2*COS(T(I))**2
      B33T=(B33T+BL*G*(COS(T(I))**2-SIN(T(I))**2)**2)/BL
      B12T=(EA+EB-4.*BL*G)*SIN(T(I))**2*COS(T(I))**2
      B12T=(B12T+EA*PB*(COS(T(I))**4+SIN(T(I))**4))/BL
      B13T=(EB-EA-PB-2.*BL*G)*SIN(T(I))**3*COS(T(I))
      B13T=(B13T-(EA-EA*PB-2.*BL*G)*SIN(T(I))*COS(T(I))**3)/BL
      B23T=(EB-EA-PB-2.*BL*G)*SIN(T(I))*COS(T(I))**3
      B23T=(B23T-(EA-EA*PB-2.*BL*G)*SIN(T(I))**3*COS(T(I)))/BL
C SUFFIX S REFERS TO TOTAL COMPOSITE
      B11S=(1.-R(N))*B110+R(N)*B11T
      B22S=(1.-R(N))*B220+R(N)*B22T
      B33S=(1.-R(N))*B330+R(N)*B33T
      B12S=(1.-R(N))*B120+R(N)*B12T
      S=B11S*B22S*B33S-B12S**2*B33S
      R11=B22S*B33S/S
      R22=B11S*B33S/S
      R33=(B11S*B22S-B12S**2)/S
      R12=(-B12S*B33S)/S
      EX=R11*SX+R12*SY
      EY=R12*SX+R22*SY
      EXY=PBS*TXY
C SX0,SY0,TXY0 ARE STRESSES IN THE 0 LAYER
      SX0=B110*EX+B120*EY
      SY0=B120*EX+B220*EY
      TXY0=B330*EXY
      WRITE(2,49)SX0,SY0,TXY0
   49 FORMAT(3E10.0)
      IF(SX0)52,50,50
C FOT IS STRENGTH FACTOR FOC FIT FCI SIMILAR
```

```
   50 FOT=150./SQRT(SX0**2-SX0*SY0+625.*SY0**2+352.*TXY0**2)
      WRITE(2,51)FOT
   51 FORMAT(5H FOT=,3PF10.0)
      GO TO 54
   52 FOC=120./SQRT(SX0**2-SX0*SY0+400.*SY0**2+225.*TXY0**2)
      WRITE(2,53)FOC
   53 FORMAT(5H FOC=,3PF10.0)
   54 SXT=B11T*EX+B12T*EY+B13T*EXY
      SYT=B12T*EX+B22T*EY+B23T*EXY
      TXYT=B13T*EX+B23T*EY+B33T*EXY
C SXT,SYT TXYT ARE STRESSES IN CROSS PLY LAYER  - θ Positive.
      WRITE(2,47)SXT,SYT,TXYT
   47 FORMAT(3F10.0)
      SA=COS(T(I))**2*SXT+SIN(T(I))**2*SYT-2.*SIN(T(I))*COS(T(I))*TXYT
      SB=SIN(T(I))**2*SXT+COS(T(I))**2*SYT+2.*SIN(T(I))*COS(T(I))*TXYT
      TAB=SIN(T(I))*COS(T(I))*SXT-SIN(T(I))*COS(T(I))*SYT
      TAB=TAB+(COS(T(I))**2-SIN(T(I))**2)*TXYT
C SA,SB,TAB ARE STRESSES IN CROSS PLY REFERED TO FILAMENT AXES
      WRITE(2,48)SA,SB,TAB
   48 FORMAT(3F10.0)
      IF(SA)57,55,55
   55 FIT=150./SQRT(SA**2-SA*SB+625.*SB**2+352.*TAB**2)
      WRITE(2,56)FIT
   56 FORMAT(5H FIT=,3PF10.0)
      GO TO 59
   57 FIC=120./SQRT(SA**2-SA*SB+400.*SB**2+255.*TAB**2)
      WRITE(2,58)FIC
   58 FORMAT(5H FIC=,3PF10.0)
   59 WRITE(2,60)I(N),T(I)
   60 FORMAT(1F6.3,1F8.4)
   62 CONTINUE
   61 CONTINUE
      STOP
      END

END OF SEGMENT, LENGTH   989, NAME  COMPOSITESTRENGTH
```

R TETLOW COMPOSITE STRENGTH

```
 1000.      0.      0.
    1007.          -3.          0.
FOT=        148.
     940.          24.       -155.
     965.          -2.         11.
FIT=        152.
0.100  0.1745
    1014.          -5.          0.
FOT=        146.
     945.          21.       -156.
     970.          -4.         12.
FIT=        150.
0.200  0.1745
    1021.          -8.          0.
FOT=        144.
     950.          19.       -156.
     975.          -7.         12.
FIT=        147.
0.300  0.1745
    1030.         -11.          0.
FOT=        140.
     955.          16.       -157.
     981.          -9.         13.
FIT=        144.
0.400  0.1745
    1038.         -13.          0.
FOT=        137.
     962.          13.       -158.
     987.         -12.         14.
FIT=        140.
0.500  0.1745
    1048.         -16.          0.
FOT=        133.
     968.          11.       -159.
     994.         -15.         14.
FIT=        136.
0.600  0.1745
    1058.         -19.          0.
FOT=        129.
     975.           8.       -160.
    1001.         -17.         15.
FIT=        132.
0.700  0.1745
    1068.         -22.          0.
FOT=        124.
     983.           5.       -161.
    1009.         -20.         16.
FIT=        128.
0.800  0.1745
    1079.         -25.          0.
FOT=        120.
     991.           3.       -162.
    1017.         -23.         17.
FIT=        123.
0.900  0.1745
    1091.         -27.          0.
FOT=        115.
    1000.           0.       -163.
    1026.         -26.         17.
FIT=        119.
1.000  0.1745
```

Typical Set of Results

For σ_x=1000.

σ_y= 0.

τ_{xy}= 0.

$\theta = 10^{o}$

TABLE 1: Efficiency Factors for Wide Columns

(Derived from ref.15, Emero and Spunt)

$$\sigma_{OPT} = F.\sqrt{E}\sqrt{\frac{\omega}{L}}$$

TYPE		F
Plain corrugation		1.26
Trapezoidal corrugated, semi sandwich		0.83
Truss core, semi sandwich	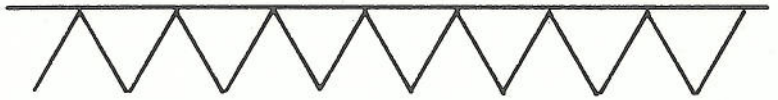	0.83
Semi trap. corrugated semi sandwich		0.85
Top hat stiffened	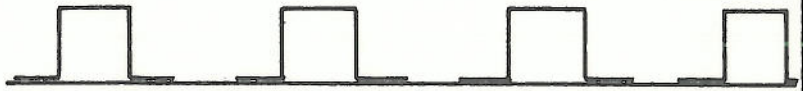	0.96
Truss core corrugation		1.07
Semicircle corrugation		0.84
Truss core sandwich	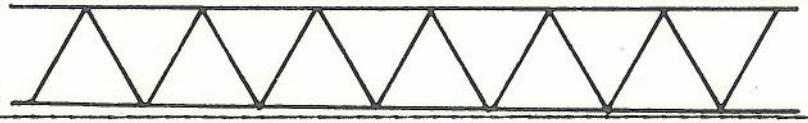	0.78

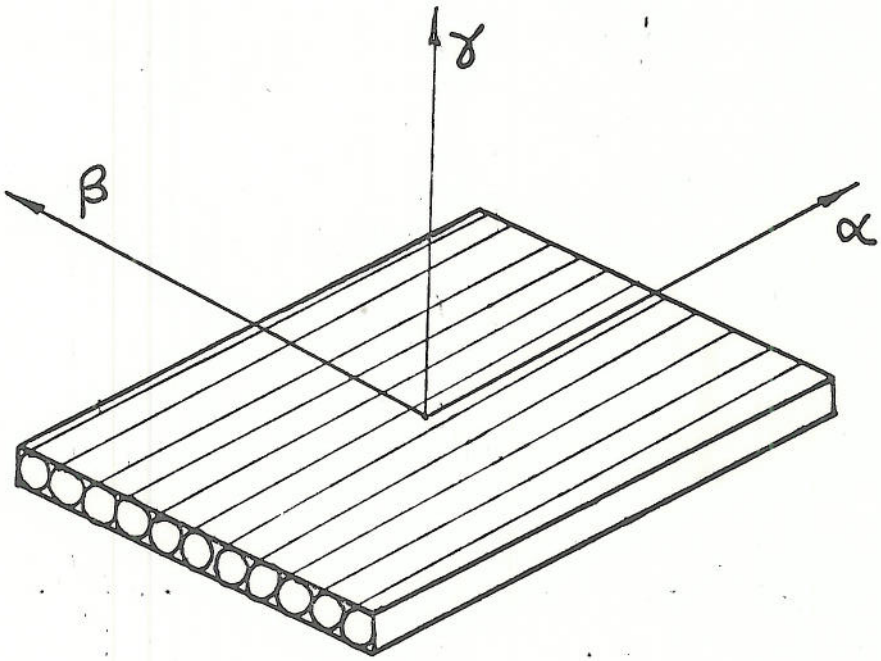

FIG. I. SINGLE UNIDIRECTIONAL PLY

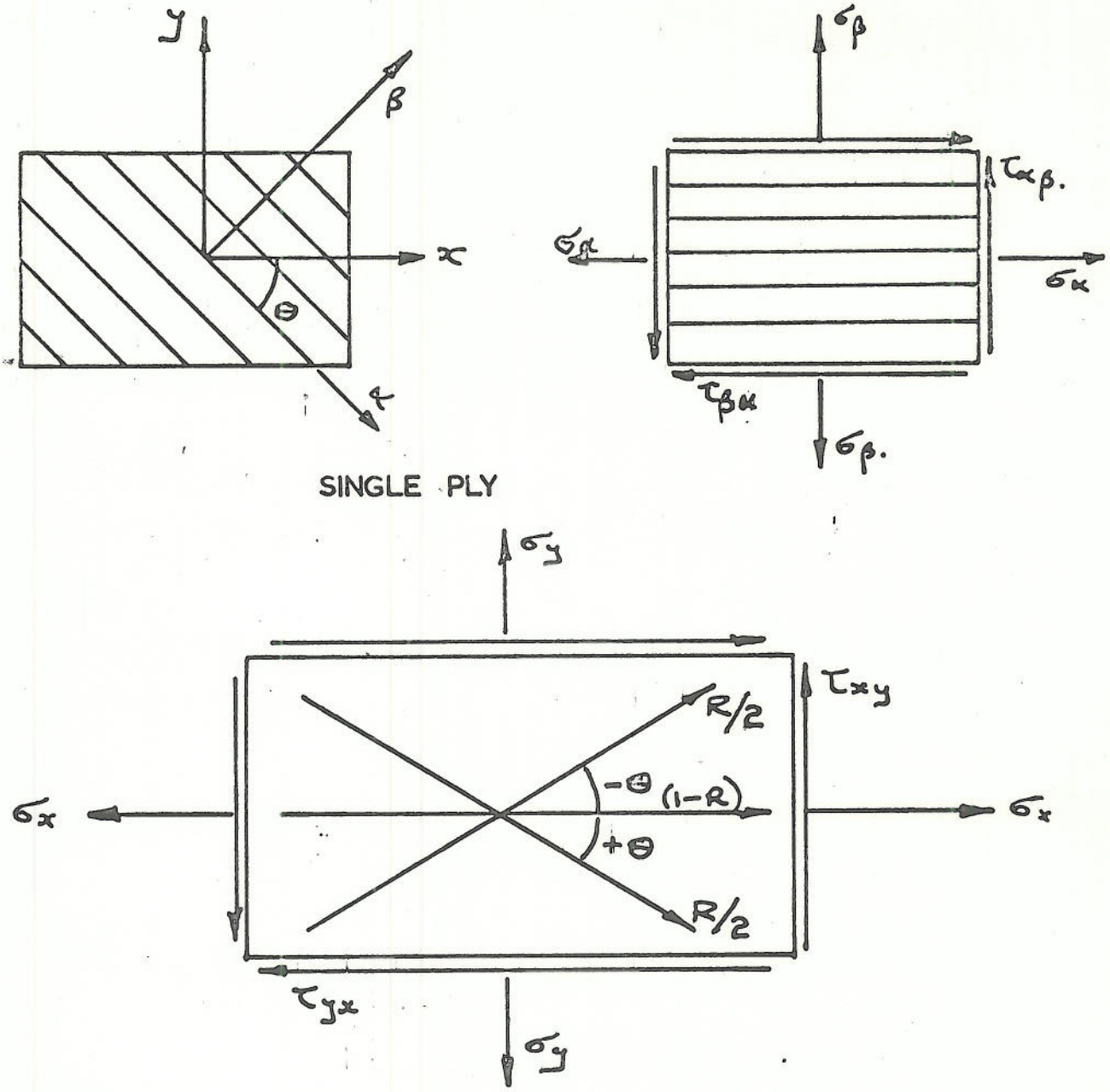

FIG. 2. SIGN CONVENTION

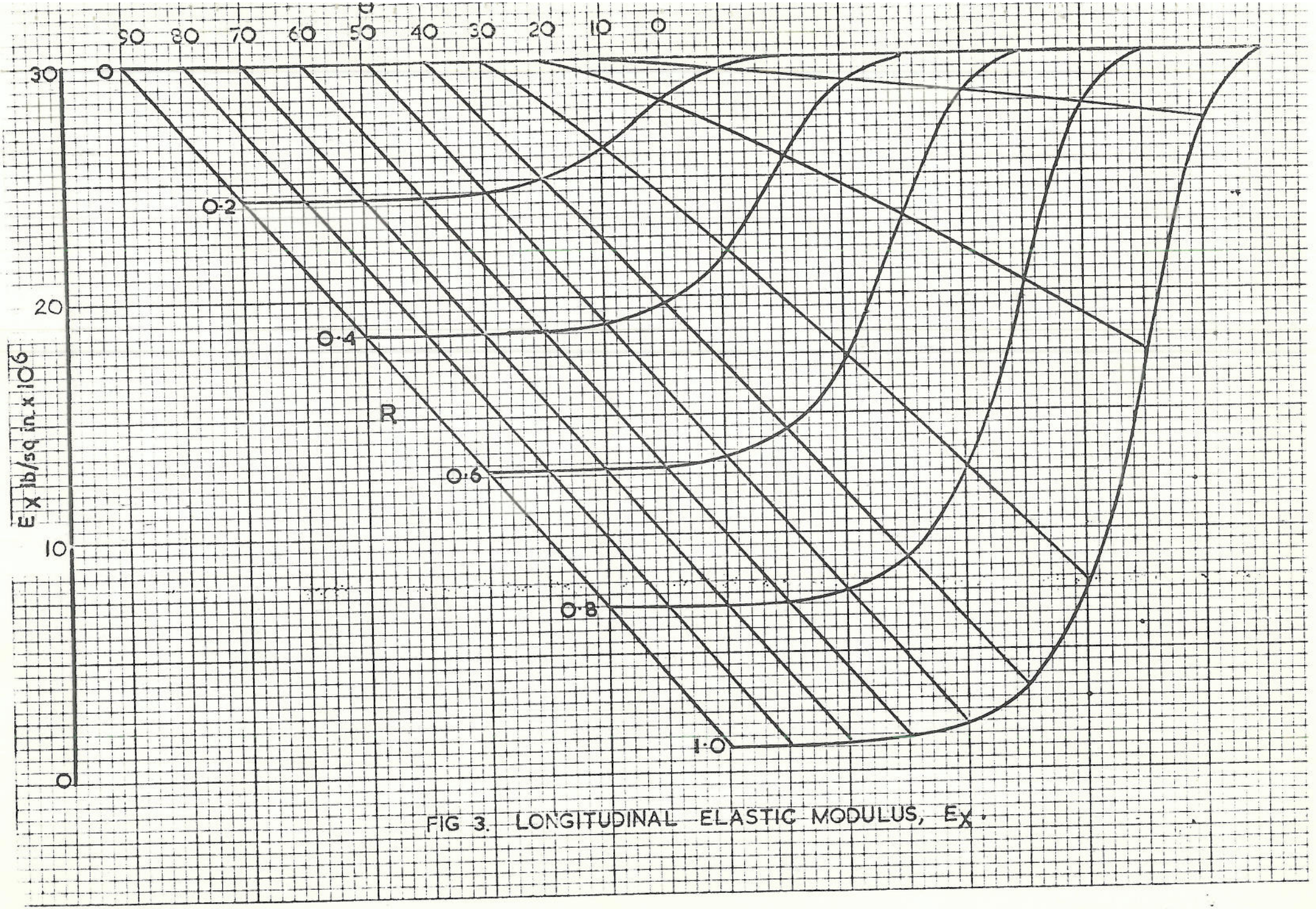

FIG 3. LONGITUDINAL ELASTIC MODULUS, E_x.

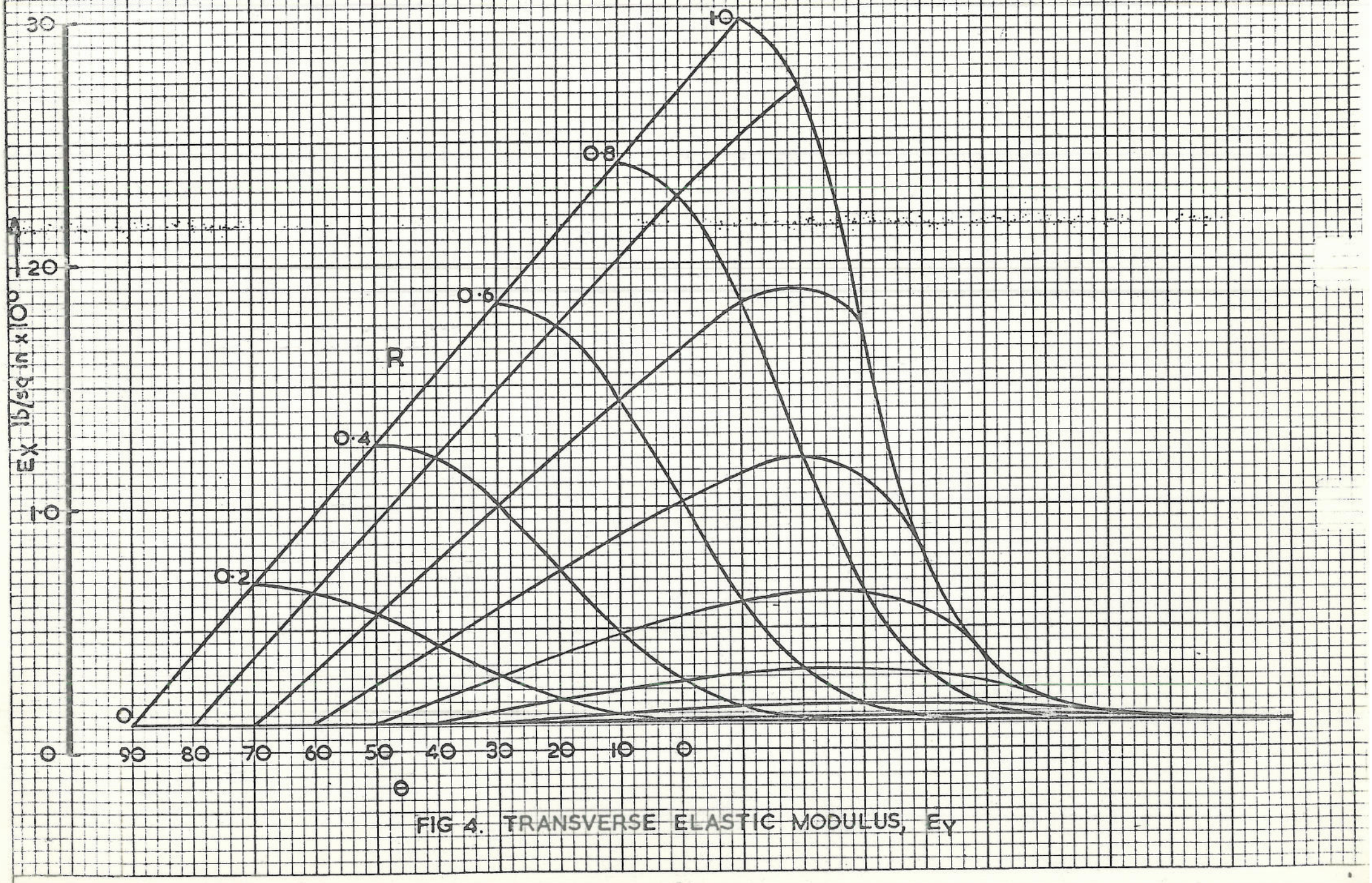

FIG 4. TRANSVERSE ELASTIC MODULUS, E_Y

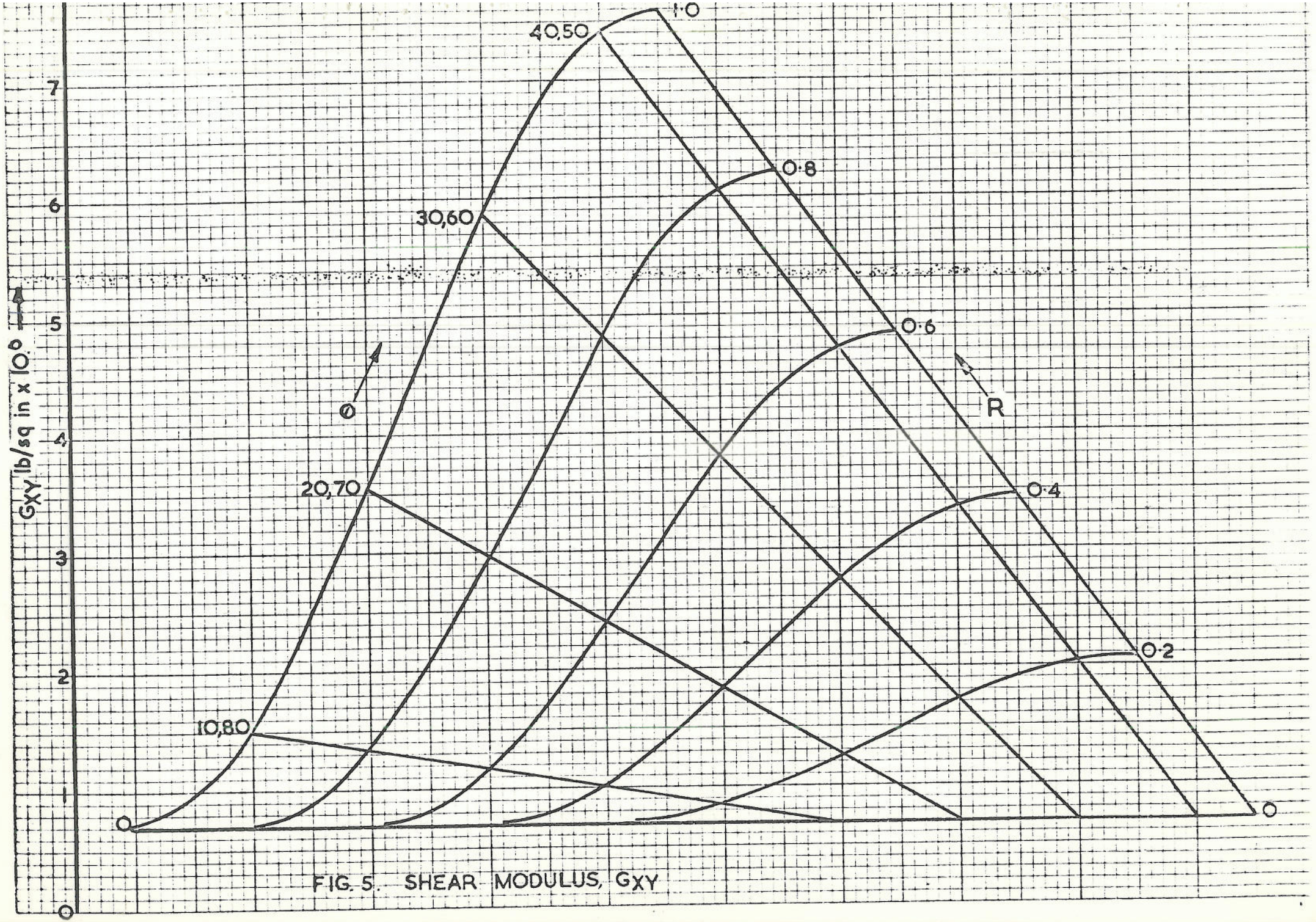

FIG. 5. SHEAR MODULUS, GXY

FIG. 6. STRENGTH CHART

(longitudinal stress only)

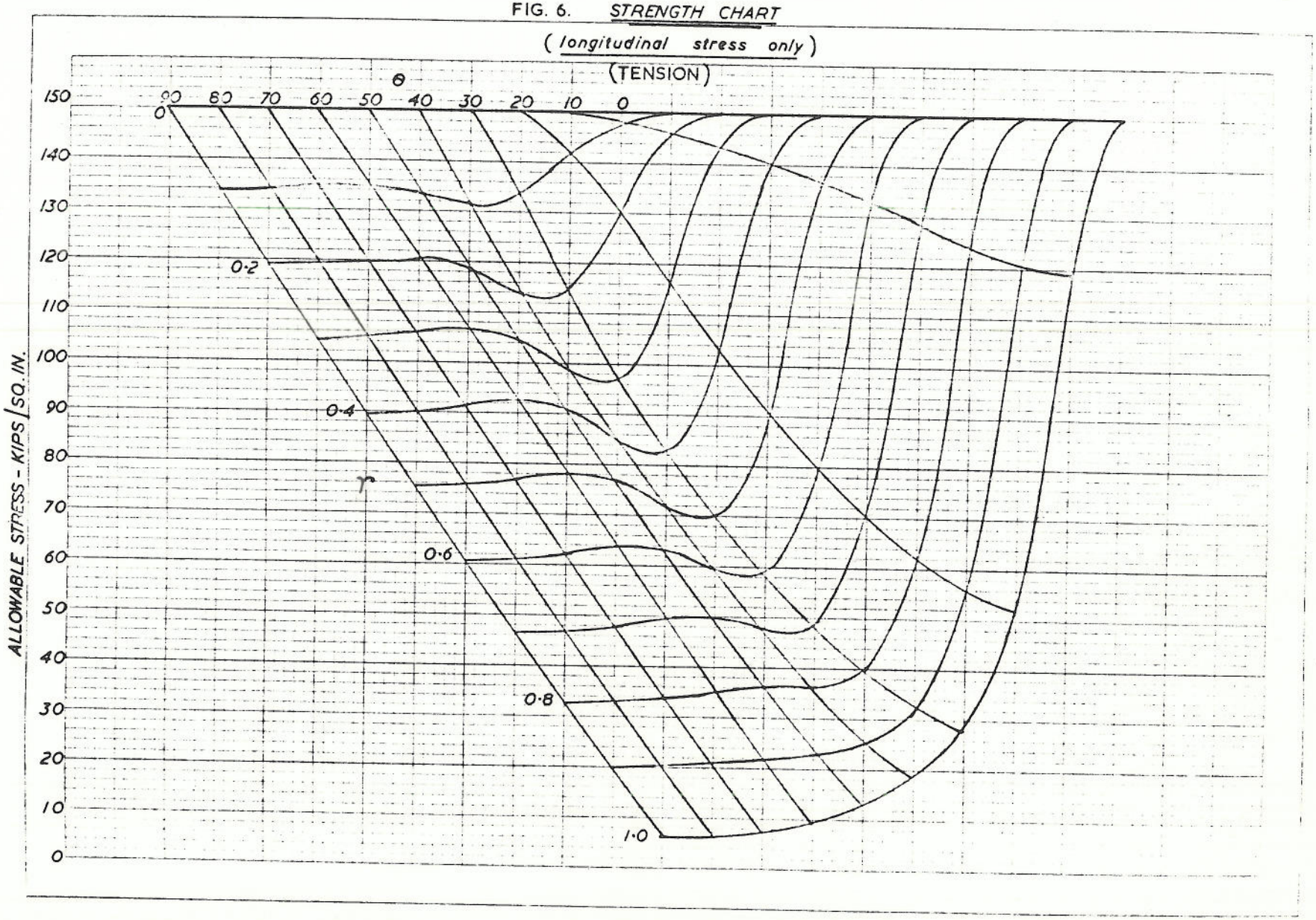

FIG. 7. STRENGTH CHART

(COMPRESSIVE STRESS ONLY)

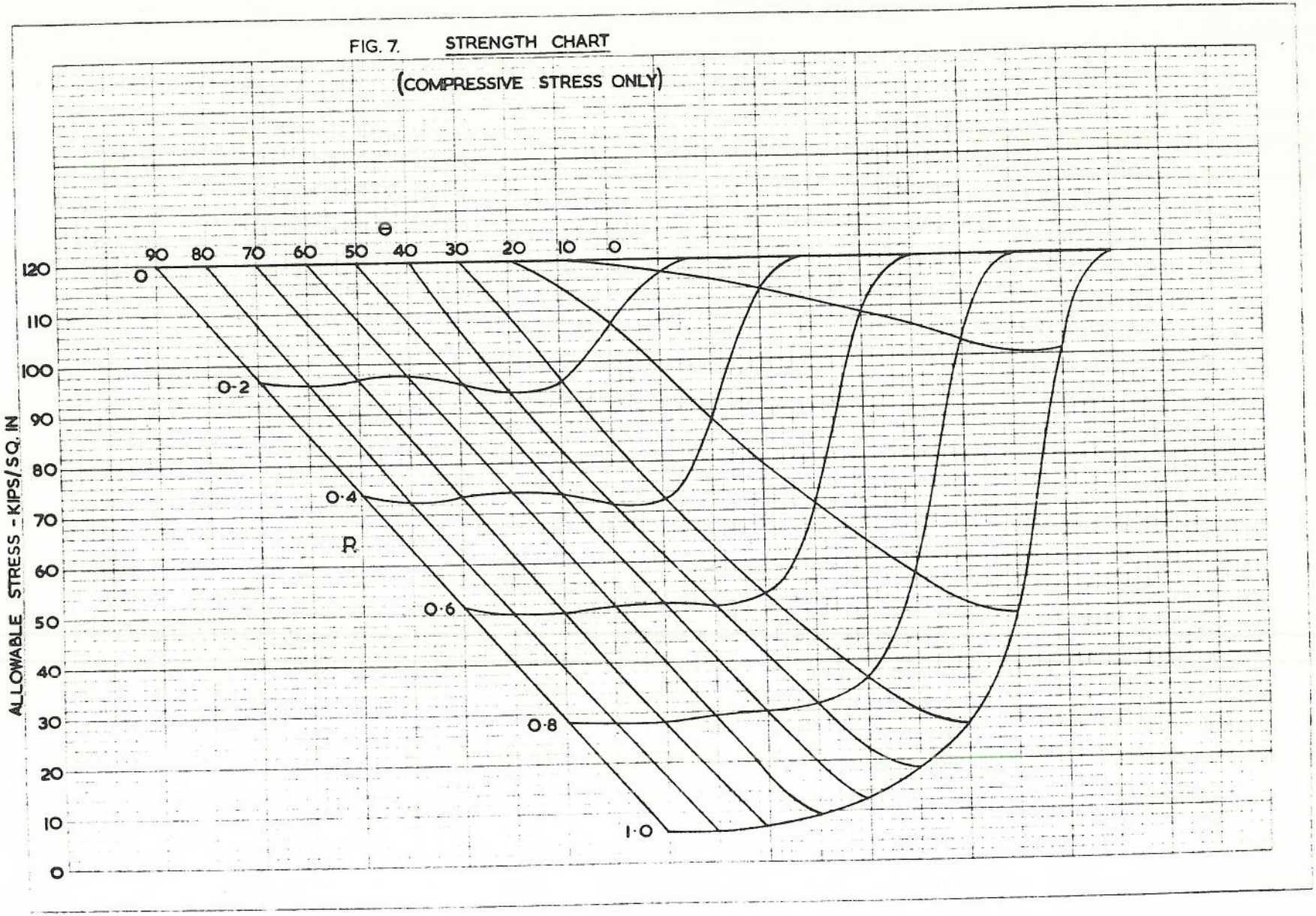

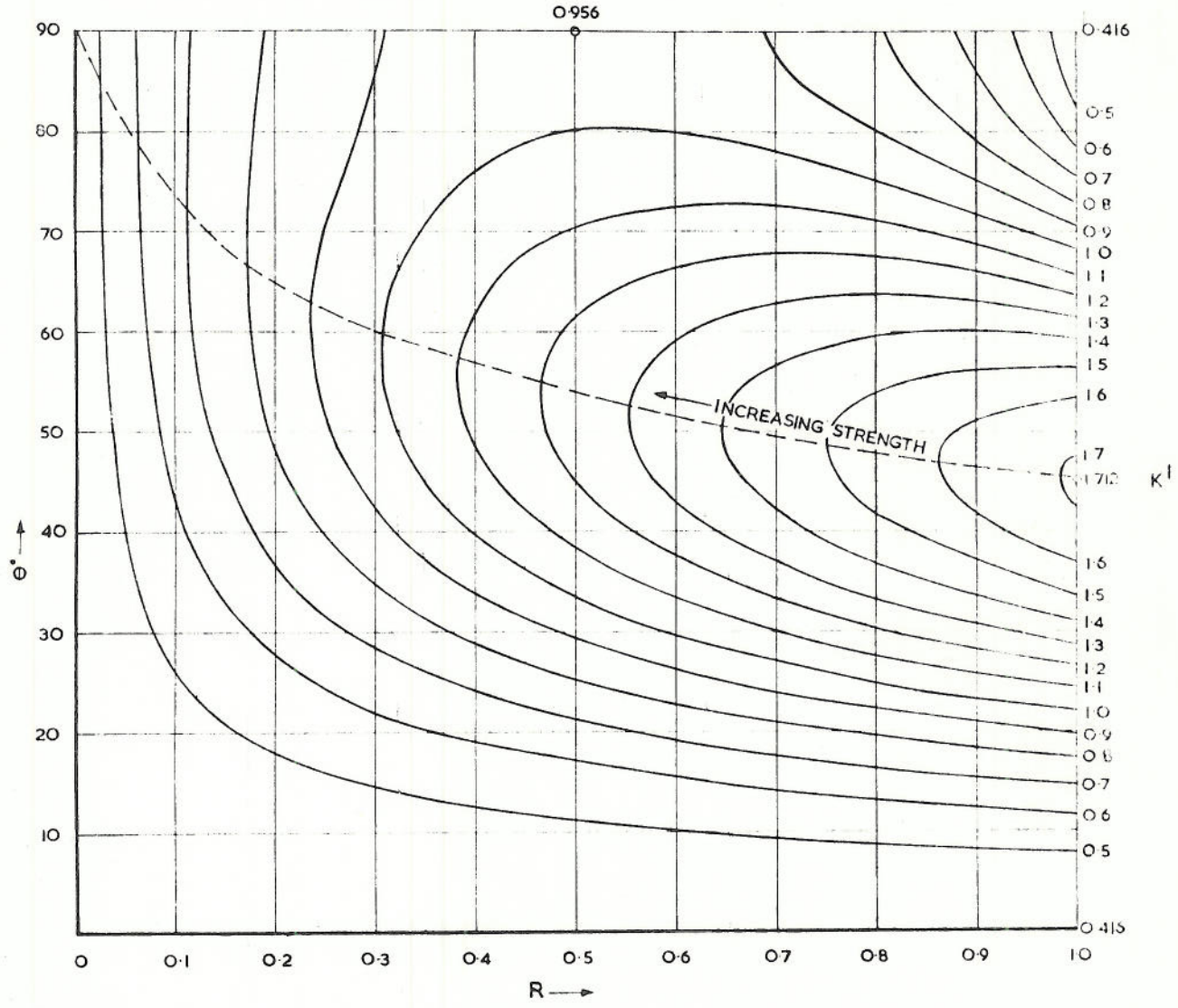

FIG. 8. SIMPLY SUPPORTED COMPRESSION PANEL, BUCKLING COEFFICIENTS

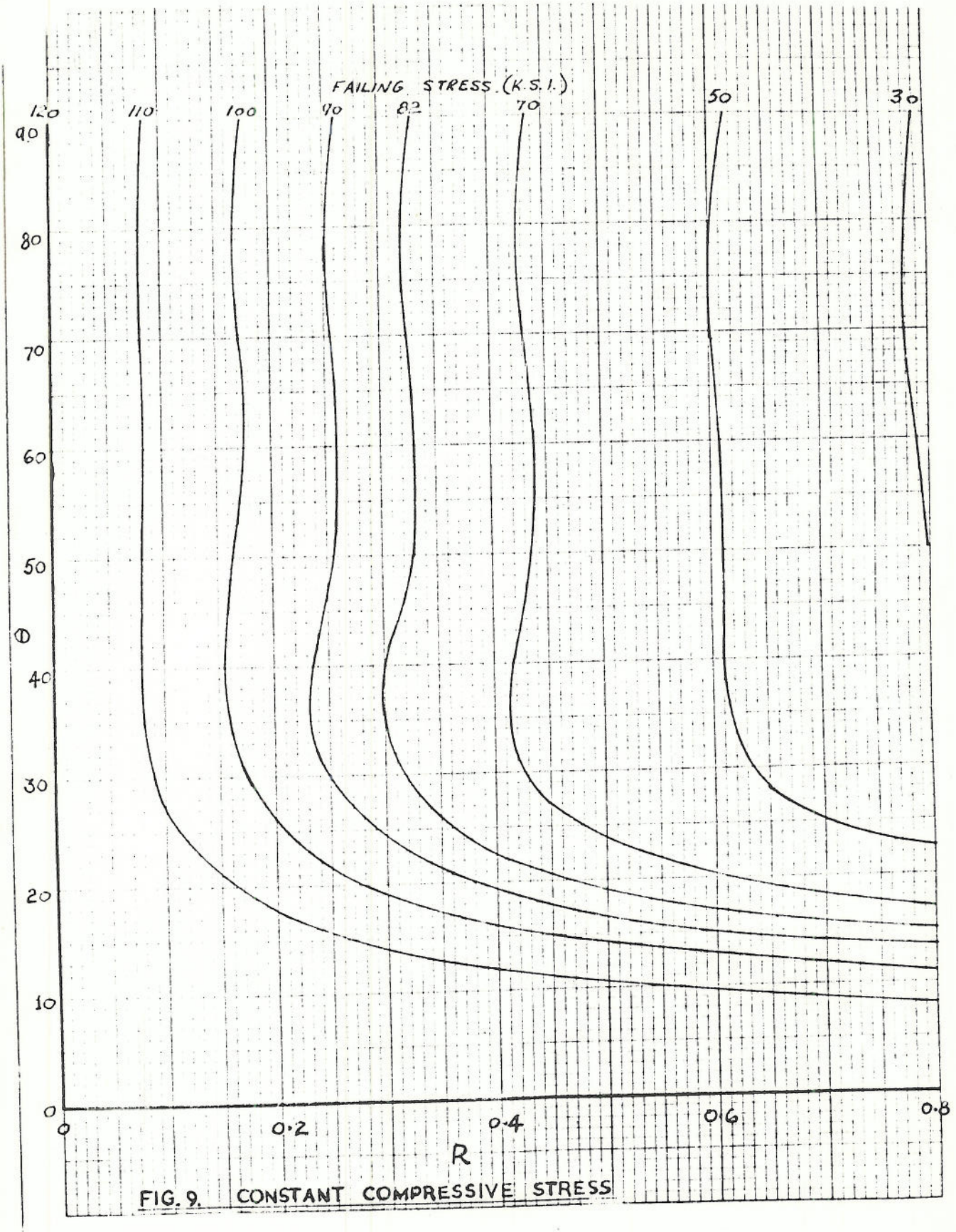

FIG. 9. CONSTANT COMPRESSIVE STRESS

FIG. 10. OPTIMUM STRESS LEVEL FOR S.S. PLATE IN COMPRESSION

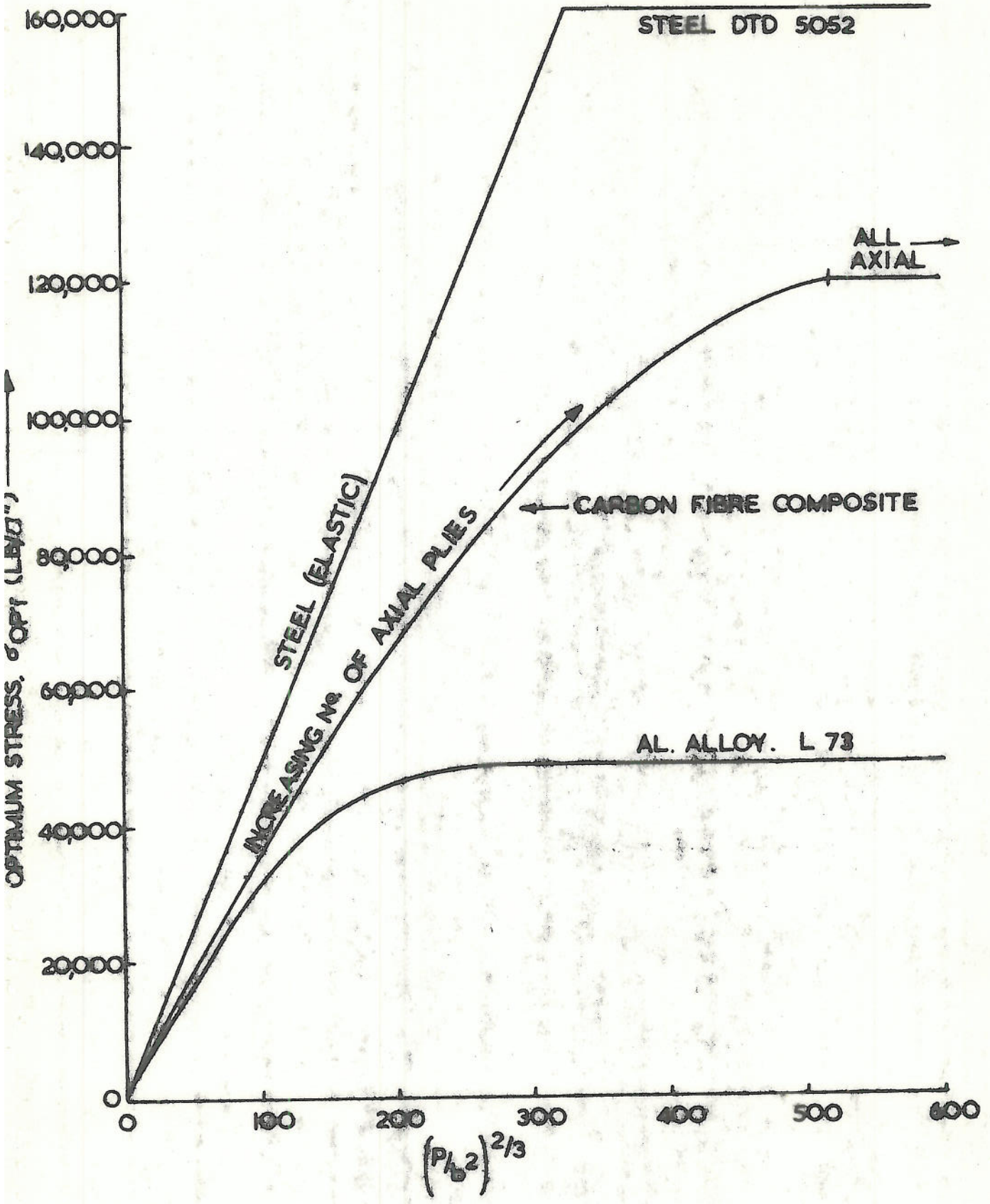

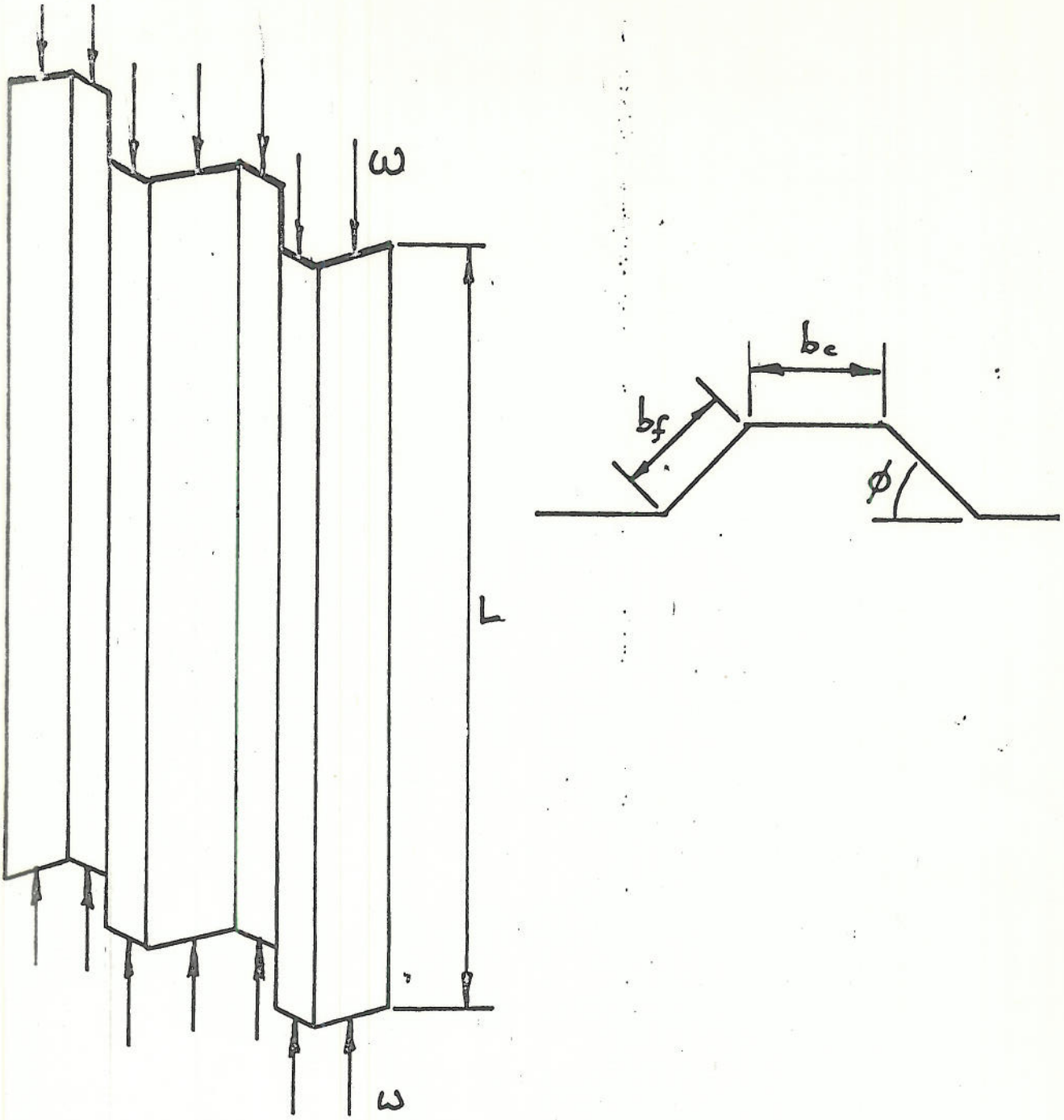

FIG. 11. CORRUGATED COMPRESSION PANEL

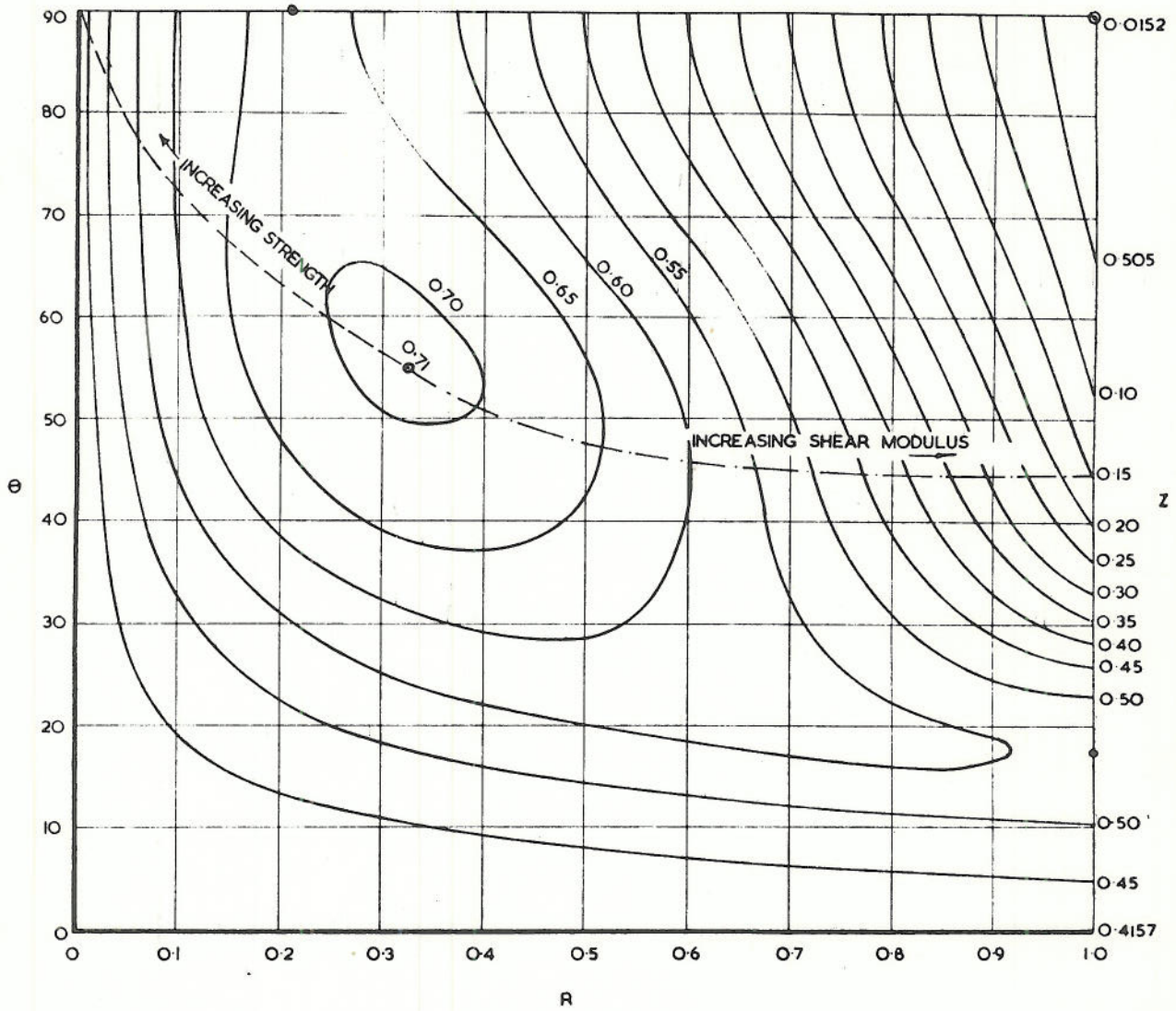

FIG 12, CORRUGATED COMPRESSION PANEL, BUCKLING CHART

FIG 13

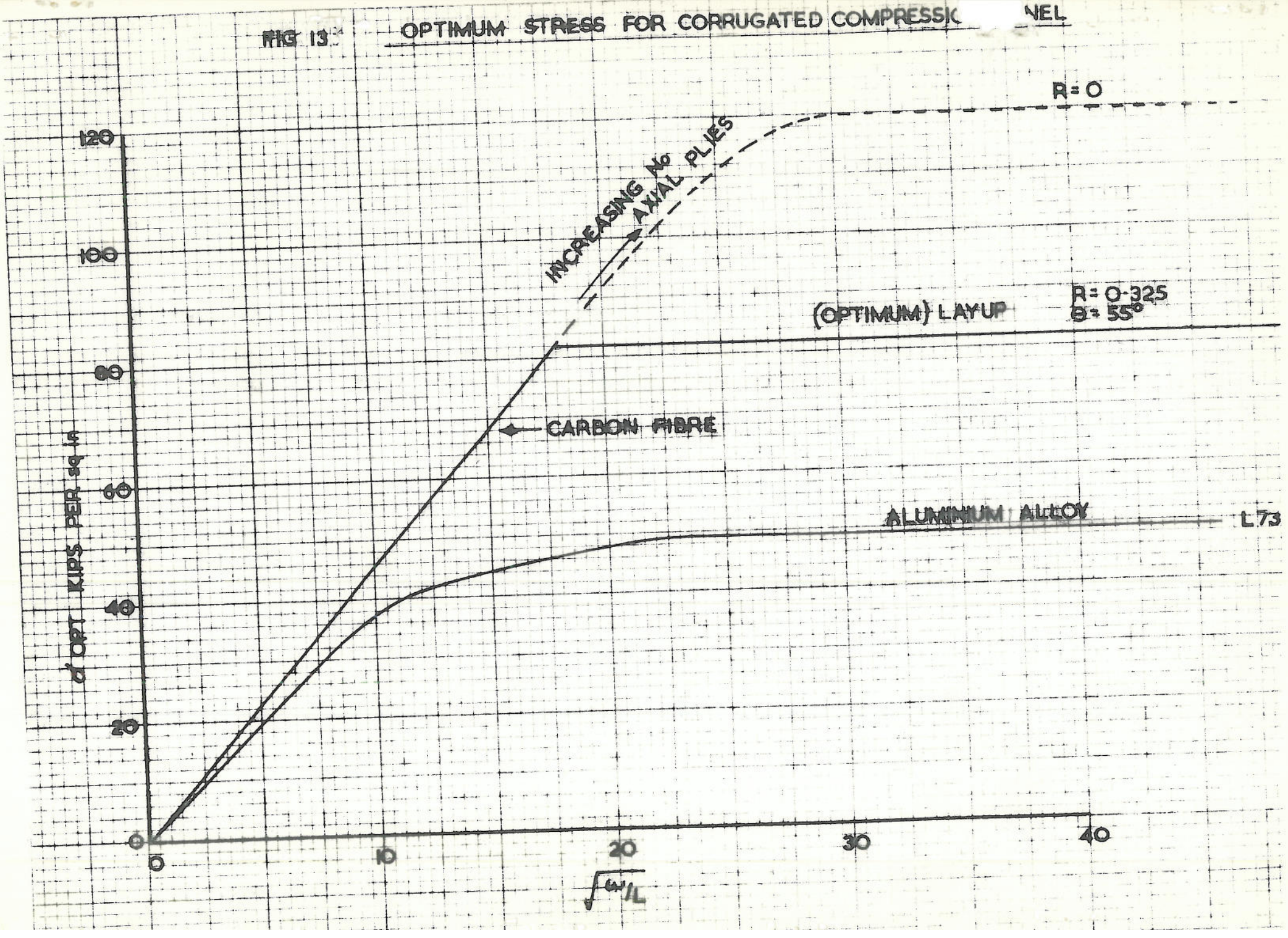
OPTIMUM STRESS FOR CORRUGATED COMPRESSION PANEL
R = 0
INCREASING No AXIAL PLIES
(OPTIMUM) LAYUP
R = 0·325
θ = 55°
CARBON FIBRE
ALUMINUM ALLOY
L73
σ' OPT KIPS PER sq in
120
100
80
60
40
20
0
0
10
20
30
40
√ω/L